Resonance in a Superstrate-Loaded Rectangular Microstrip Structure

Jeen-Sheen Row and Kin-Lu Wong, *Member, IEEE*

***Abstract*— The complex resonant frequency of a superstrate-loaded rectangular microstrip structure is investigated. The study is performed by using a full-wave analysis and Galerkin's moment method. The numerical convergence using sinusoidal basis functions, with and without considering the edge singularity to expand the unknown surface current distribution on the rectangular patch, is discussed. Numerical results for the effects of superstrate permittivity and thickness on the complex resonant frequency of the rectangular microstrip structure are also presented.**

I. Introduction

The complex resonant frequency problem of a rectangular microstrip patch has been recently studied in [1], where an accurate method of determining the resonant frequency of the rectangular microstrip structure is shown. In this paper, we extend the study to the case of a superstrate-loaded rectangular microstrip structure, where the superstrate layer loaded on the microstrip structure is often imposed by design to protect the microstrip patch antenna from environmental hazards [2]–[4]. The study here is also based on a rigorous full-wave analysis and Galerkin's moment method [5]. Two different sets of sinusoidal basis functions are used to expand the unknown surface current distribution on the rectangular patch, one of which takes into account the edge singularity condition. The numerical convergence for these two different sets of basis functions is discussed in detail. The effects of superstrate loading on the real and imaginary parts of the complex resonant frequency of the rectangular microstrip structure are also presented.

II. Theoretical Formulation of the Problem

The geometry for the superstrate-loaded rectangular microstrip structure is illustrated in Fig. 1. The patch is located on a grounded substrate (region 1) of thickness d having relative permittivity ε_1. On the top of the substrate is the superstrate (region 2) of thickness t with relative permittivity ε_2. Above the superstrate is free space (region 3) with permittivity ε_0. The permeability is everywhere assumed to be μ_0. For the analysis of the resonance problem, the transverse electric fields at $z = d$ are considered. Plane wave solutions proportional to $e^{j\omega t}$ are assumed in the following theoretical treatment. The transverse electric fields due to the surface currents $\vec{J}_x$ and $\vec{J}_y$ on the patch can be expressed as

$$\vec{E}_x = \hat{x}\frac{1}{4\pi^2}\int_{-\infty}^{\infty}\int_{-\infty}^{\infty}(Q_{xx}F_x + Q_{xy}F_y)\cdot\exp(jk_x x + jk_y y)\,dk_x\,dk_y \tag{1a}$$

$$\vec{E}_y = \hat{y}\frac{1}{4\pi^2}\int_{-\infty}^{\infty}\int_{-\infty}^{\infty}(Q_{yx}F_x + Q_{yy}F_y)\cdot\exp(jk_x x + jk_y y)\,dk_x\,dk_y \tag{1b}$$

where F_x and F_y are the Fourier transforms of J_x and J_y, respectively; Q_{xx}, Q_{xy}, Q_{yx}, and Q_{yy} are the elements of the dyadic Green's function at $z = d$ for a grounded substrate covered with a superstrate. These elements are found to be

$$Q_{xx} = \frac{-j}{\omega\varepsilon_0}\left[\frac{k_x^2 k_1\sin(k_1 d)}{\beta^2 T_m}D_m + \frac{k_y^2 k_0^2\sin(k_1 d)}{\beta^2 T_e}D_e\right]$$
$$Q_{yy} = \frac{-j}{\omega\varepsilon_0}\left[\frac{k_y^2 k_1\sin(k_1 d)}{\beta^2 T_m}D_m + \frac{k_x^2 k_0^2\sin(k_1 d)}{\beta^2 T_e}D_e\right]$$
$$Q_{xy} = \frac{-j}{\omega\varepsilon_0}\left[\frac{k_x k_y k_1\sin(k_1 d)}{\beta^2 T_m}D_m - \frac{k_x k_y k_0^2\sin(k_1 d)}{\beta^2 T_e}D_e\right]$$
$$Q_{yx} = Q_{xy}$$

where

$$T_m = \cos(k_2 t)[\varepsilon_1 k_3\cos(k_1 d) + jk_1\sin(k_1 d)] + j\sin(k_2 t)\left[\frac{\varepsilon_1}{\varepsilon_2}k_2\cos(k_1 d) + j\frac{\varepsilon_2 k_1 k_3}{k_2}\sin(k_1 d)\right]$$
$$T_e = \cos(k_2 t)[k_1\cos(k_1 d) + jk_3\sin(k_1 d)] + j\sin(k_2 t)\left[\frac{k_1 k_3}{k_2}\cos(k_1 d) + jk_2\sin(k_1 d)\right]$$
$$D_m = k_3\cos(k_2 t) + j\frac{k_2}{\varepsilon_2}\sin(k_2 t)$$
$$D_e = \cos(k_2 t) + j\frac{k_3}{k_2}\sin(k_2 t)$$
$$k_i^2 = \varepsilon_i k_0^2 - \beta^2, \qquad i = 1,2,3; \quad \varepsilon_3 = 1.0$$
$$\beta^2 = k_x^2 + k_y^2, \qquad k_0^2 = \omega^2\mu_0\varepsilon_0\,.$$

The first subscript on Q represents the field direction while the second subscript shows the dipole orientation. Since the resonant frequency is defined to be the frequency at which the field and the current can sustain themselves without an external source, the transverse electric fields of (1a) and (1b) must necessarily be zero on the perfectly conducting patch at

Manuscript received June 29, 1992; revised December 14, 1992. This work was supported by the National Science Council of the Republic of China under Grant NSC81-0404-E110-544.

The authors are with the Department of Electrical Engineering, National Sun Yat-Sen University, Kaohsiung, Taiwan 804, Republic of China.

IEEE Log Number 9210208.

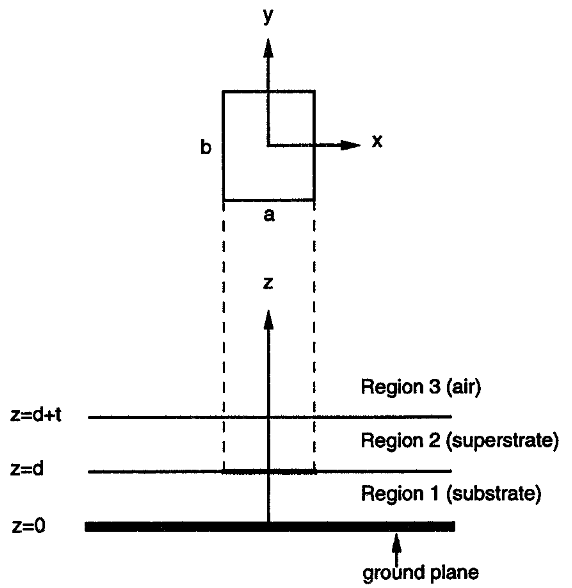

Fig. 1. Rectangular patch in a substrate-superstrate geometry.

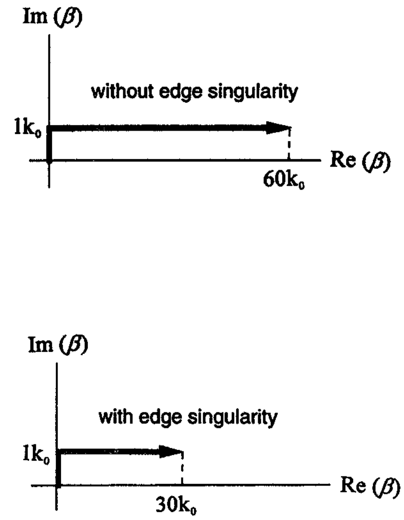

Fig. 2. The integration paths in the complex plane for the sinusoidal basis functions with and without the edge singularity condition.

resonance, i.e.,

$$\int_{-\infty}^{\infty}\int_{-\infty}^{\infty}(Q_{xx}F_x+Q_{xy}F_y)\exp(jk_xx+jk_yy)\,dk_x\,dk_y=0 \tag{2a}$$

$$\int_{-\infty}^{\infty}\int_{-\infty}^{\infty}(Q_{yx}F_x+Q_{yy}F_y)\exp(jk_xx+jk_yy)\,dk_x\,dk_y=0 \tag{2b}$$

The procedure for solving the above equations is based on Galerkin's method [5]. The unknown surface current components J_x and J_y, whose Fourier transforms are F_x and F_y, are expanded in terms of linear combinations of known basis functions, i.e.,

$$J_x(x,y)=\sum_{n=1}^{N}a_nJ_{xn}(x,y) \tag{3a}$$

$$J_y(x,y)=\sum_{m=1}^{M}b_mJ_{ym}(x,y). \tag{3b}$$

Substituting the Fourier transforms of (3) into (2) and taking the symmetric products of the resulting equations with each basis function, we can have the following homogeneous matrix equation:

$$\begin{bmatrix}(Z_{kn}^{xx})_{N\times N} & (Z_{km}^{xy})_{N\times M}\\ (Z_{ln}^{yx})_{M\times N} & (Z_{lm}^{yy})_{M\times M}\end{bmatrix}\begin{bmatrix}(a_n)_{N\times 1}\\ (b_m)_{M\times 1}\end{bmatrix}=\begin{bmatrix}0\\0\end{bmatrix} \tag{4}$$

where

$$Z_{kn}^{xx}=\int_{-\infty}^{\infty}\int_{-\infty}^{\infty}F_{xk}(-k_x,-k_y)\cdot Q_{xx}F_{xn}(k_x,k_y)\,dk_x\,dk_y \tag{5a}$$

$$Z_{km}^{xy}=\int_{-\infty}^{\infty}\int_{-\infty}^{\infty}F_{xk}(-k_x,-k_y)\cdot Q_{xy}F_{ym}(k_x,k_y)\,dk_x\,dk_y \tag{5b}$$

$$Z_{ln}^{yx}=\int_{-\infty}^{\infty}\int_{-\infty}^{\infty}F_{yl}(-k_x,-k_y)\cdot Q_{yx}F_{xn}(k_x,k_y)\,dk_x\,dk_y \tag{5c}$$

$$Z_{lm}^{yy}=\int_{-\infty}^{\infty}\int_{-\infty}^{\infty}F_{yl}(-k_x,-k_y)\cdot Q_{yy}F_{ym}(k_x,k_y)\,dk_x\,dk_y \tag{5d}$$

$$k,n=1,2,3,\cdots,N,\qquad l,m=1,2,3,\cdots,M.$$

Since the quantities Z_{kn}^{xx}, etc., are functions of complex frequencies and the existence of nontrivial solutions for a_m and b_n requires that

$$\det[Z]=0. \tag{6}$$

where Z is the matrix in (4), the resonance solutions are satisfied by complex frequencies. In choosing the set of basis functions for solving (6), the unknown surface current density on the patch can be expanded by the following sinusoidal basis functions:

$$J_{xn}=\sin\left[\frac{p\pi}{a}\left(x+\frac{a}{2}\right)\right]\cos\left[\frac{q\pi}{b}\left(y+\frac{b}{2}\right)\right] \tag{7a}$$

$$J_{ym}=\sin\left[\frac{r\pi}{b}\left(y+\frac{b}{2}\right)\right]\cos\left[\frac{s\pi}{a}\left(x+\frac{a}{2}\right)\right] \tag{7b}$$

or

$$J_{xn}=\sin\left[\frac{p\pi}{a}\left(x+\frac{a}{2}\right)\right]\cos\left[\frac{q\pi}{b}\left(y+\frac{b}{2}\right)\right]\cdot\frac{1}{\sqrt{\left(\frac{b}{2}\right)^2-y^2}} \tag{8a}$$

$$J_{ym}=\sin\left[\frac{r\pi}{b}\left(y+\frac{b}{2}\right)\right]\cos\left[\frac{s\pi}{a}\left(x+\frac{a}{2}\right)\right]\cdot\frac{1}{\sqrt{\left(\frac{a}{2}\right)^2-x^2}}. \tag{8b}$$

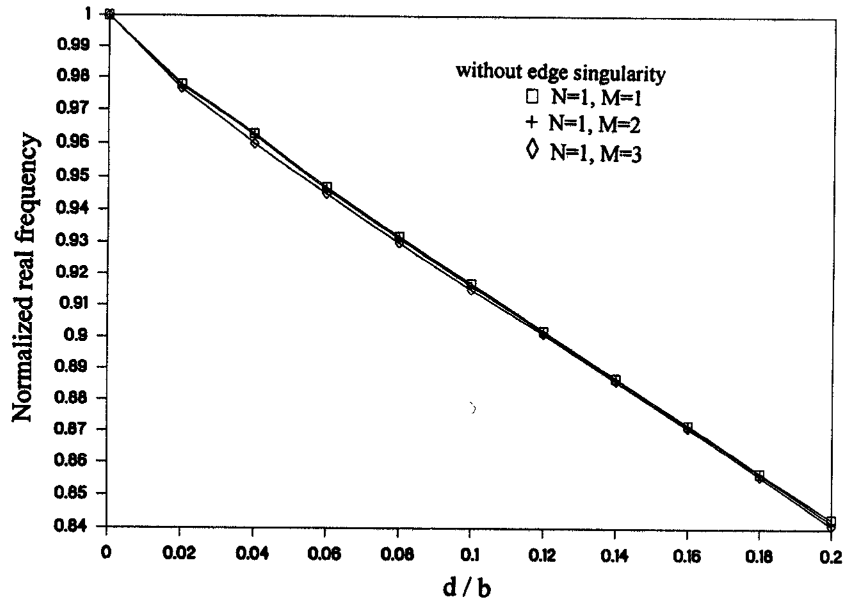

(a)

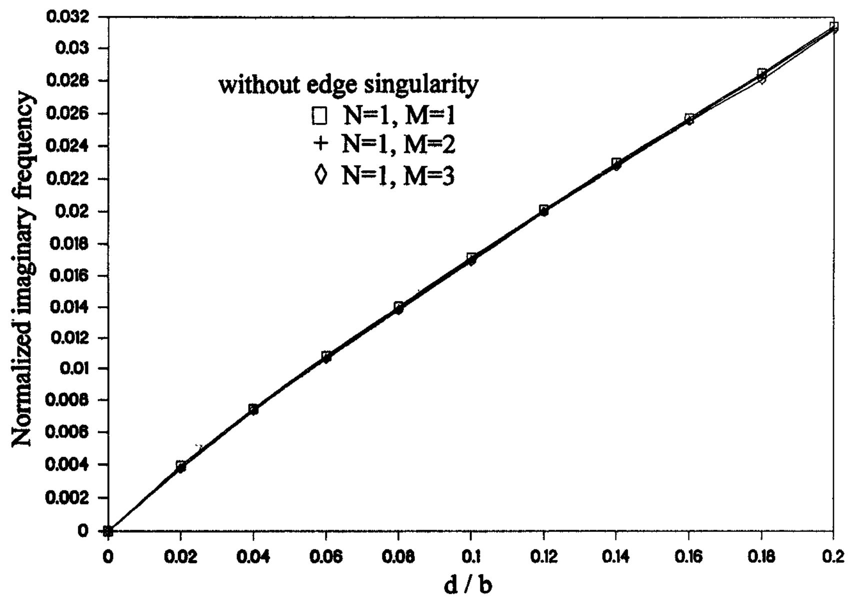

(b)

Fig. 3. Normalized resonant frequency using sinusoidal basis functions without the edge singularity versus the substrate thickness; $\varepsilon_1 = 2.3$, $a = 1.5$ cm, $b = 1$ cm, $t = 0$. (a) Real part of resonant frequency. (b) Imaginary part of resonant frequency.

The basis functions of (8), unlike those in (7), take into consideration the edge singularity condition for the tangential component of the surface current at the edge of the rectangular patch. The numerical results for the above two different basis functions are discussed in detail in the next section. The complex resonant frequencies obtained for typical superstrate-loaded microstrip structures are also presented.

III. Numerical Results and Discussion

In the evaluation of the matrix elements of (5), the double infinite integrals are changed from the (k_x, k_y) coordinates to the polar coordinates (β, α), i.e.,

$$\int_{-\infty}^{\infty}\int_{-\infty}^{\infty} dk_x\, dk_y = \int_0^{\infty}\int_0^{2\pi} \beta\, d\alpha\, d\beta. \tag{9}$$

It is also noted that the integrands are singular when T_e or T_m is zero. These singularities are poles that correspond to TE or TM surface waves. Because of radiation damping, only a complex frequency $f = f_r + jf_i$ can satisfy the system equation (6). It is necessary to evaluate the integral in the complex plane. In order to include these poles which are slightly above the real axis (for $e^{j\omega t}$ formulation), the integral is calculated along a straight path above the real axis with

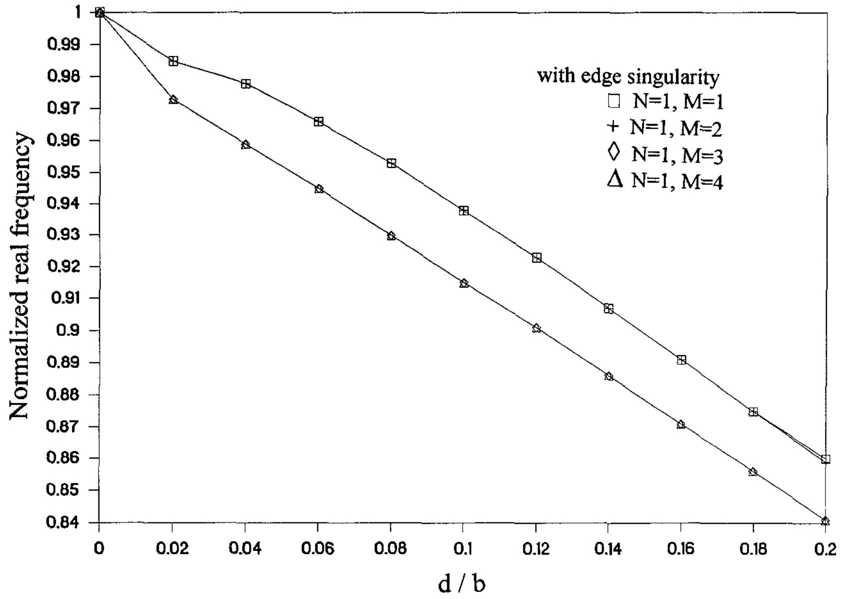

(a)

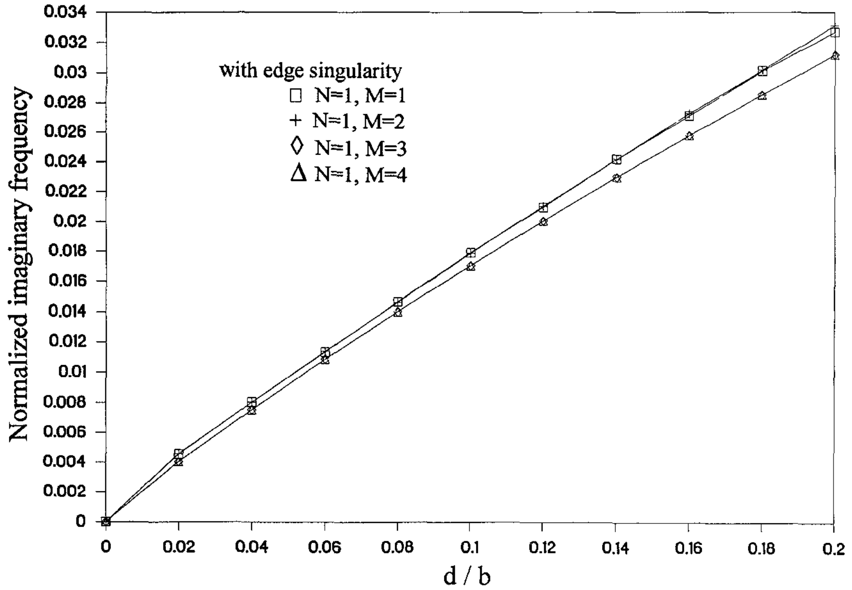

(b)

Fig. 4. Normalized resonant frequency using sinusoidal basis functions with the edge singularity versus the substrate thickness; $\varepsilon_1 = 2.3$, $a = 1.5$ cm, $b = 1$ cm, $t = 0$. (a) Real part of resonant frequency. (b) Imaginary part of resonant frequency.

a height of about $1k_0$ as shown in Fig. 2. In this case, the effects of the surface waves are included in the calculation, and no knowledge of the pole locations is required [6], while the length of the integration path is decided upon by the convergence of the numerical results. The CPU time required to compute the integral depends on the length of the integration path. It is found that the length of the integration path required to reach numerical convergence when the sinusoidal basis functions with the edge singularity are used is about half of that required when the sinusoidal basis functions without the edge singularity are used. Figs. 3 and 4 show the real and imaginary parts of the complex resonant frequencies versus the substrate thickness as obtained for different numbers of sinusoidal basis functions without and with the edge singularity. The substrate has a relative permittivity of 2.3 and the patch dimension is 1.5 cm × 1 cm. The TM_{01} mode is studied, and the frequency is normalized with respect to the cavity-model resonant frequency. In the calculation, $N = 1$ and M is varied form 1 to 4. (The case of $N = 1$, $M = 4$ is not shown in Fig. 3). From the results in Fig. 3, good convergent solutions are reached by using only two sinusoidal basis functions ($N = 1$, $M = 1$) without the edge singularity. However, as seen in Fig. 4, convergence is slow when the sinusoidal basis functions with the edge singularity are used. To reach

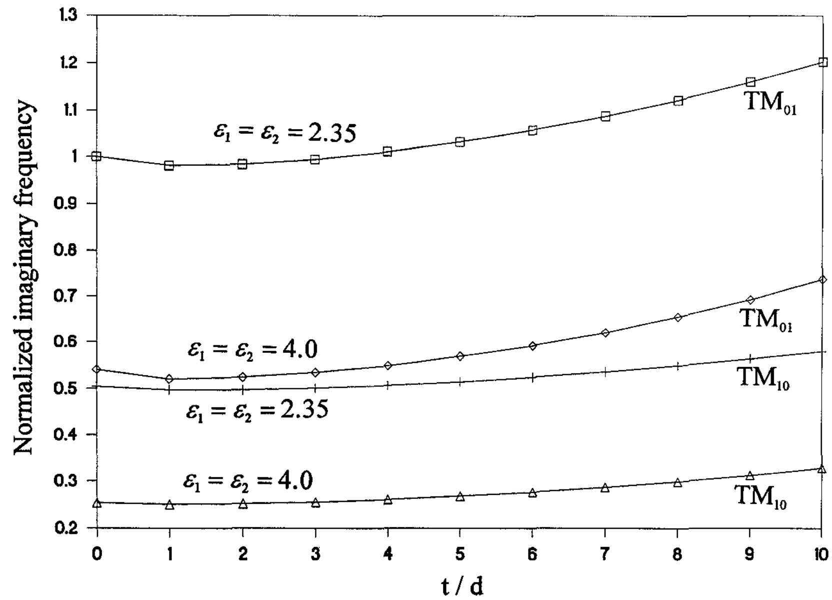

Fig. 5. Imaginary part of the normalized complex resonant frequency of a superstrate-loaded rectangular microstrip structure for TM_{01} and TM_{10} modes; $a = 6$ cm, $b = 5$ cm, $d = 0.1$ cm.

convergent solutions, four basis functions ($N = 1$, $M = 3$) with the edge singularity need to be used. Although the sinusoidal expansion functions with the edge condition require a shorter path of integration to reach numerical convergence, their use is deemed unnecessary. Similar results have also been reported in [1], where the Chebyshev polynomials with the edge singularity are used as basis functions. It should be noted that the results for which $N = 1$ and $M = 3$ in Figs. 3 and 4 are nearly the same. These convergent solutions are in good agreement with the curve-fitting results presented in [1]. Since the curve for which $N = 1$ and $M = 3$ in Fig. 3 is close to that for which $N = 1$ and $M = 1$ therein, the sinusoidal basis functions without the edge singularity with $N = 1$ and $M = 1$ are used for the rest of the study. This reduces the computation time. In this case, the computation time for reaching the convergent solution of one resonant frequency is estimated to be about 250 s on an HP720 workstation.

Fig. 5 shows the imaginary part of the normalized complex resonant frequency for the first two fundamental modes TM_{10} and TM_{01} of a superstrate-loaded rectangular microstrip structure. In Fig. 5, all the frequencies are normalized with respect to that of the TM_{01} mode with no superstrate ($t = 0$) when $\varepsilon_1 = 2.35$. The imaginary part of the resonant frequency indicates the radiation loss of the structure. The cases for which $\varepsilon_1 = \varepsilon_2 = 2.35$ and 4.0 are shown. The patch dimension is 6 cm $\times$ 5 cm. The results show that the TM_{01} mode radiates most efficiently. By comparing the results of the TM_{01} mode for the cases where $\varepsilon_1 = \varepsilon_2 = 2.35$ and 4.0, it is seen that the radiation efficiency is lower for the higher dielectric constants. This is probably due to the associated surface wave effects in substrate-superstrate layers [7], [8].

In Fig. 6, the complex resonant frequency versus the superstrate thickness for different dielectric constants of the superstrate is shown. It is observed that when the superstrate thickness is increased, the real part of the complex resonant frequency decreases monotonically. It is also seen that this decrease lessens as the superstrate permittivity decreases. For $\varepsilon_2 = 1.5$, the real part of the resonant frequency remains almost constant once the superstrate thickness exceeds about three times the substrate thickness. However, for $\varepsilon_2 = 5.6$, the real part of the resonant frequency is still decreasing when the superstrate thickness is $10d$. The resonant frequency is therefore easier to be stabilized when a superstrate of low permittivity, particularly when it is lower than that of the substrate, is placed on the top of the patch. The variation of the imaginary part of the complex resonant frequency is very small for t less than $5d$. As the superstrate thickness increases ($t > 5d$), the variation becomes significant for high superstrate permittivities.

IV. Conclusions

A rigorous analysis is presented to obtain the complex resonant frequency of the superstrate-loaded rectangular microstrip structure. The numerical convergence for the sinusoidal basis functions, with or without considering the edge singularity condition, is investigated for a rectangular patch. Results indicate that it is not necessary to consider the edge singularity to obtain fast numerical convergence of the complex resonant frequency for a rectangular microstrip structure. The obtained results show that the complex resonant frequency varies more significantly when the superstrate permittivity is greater than

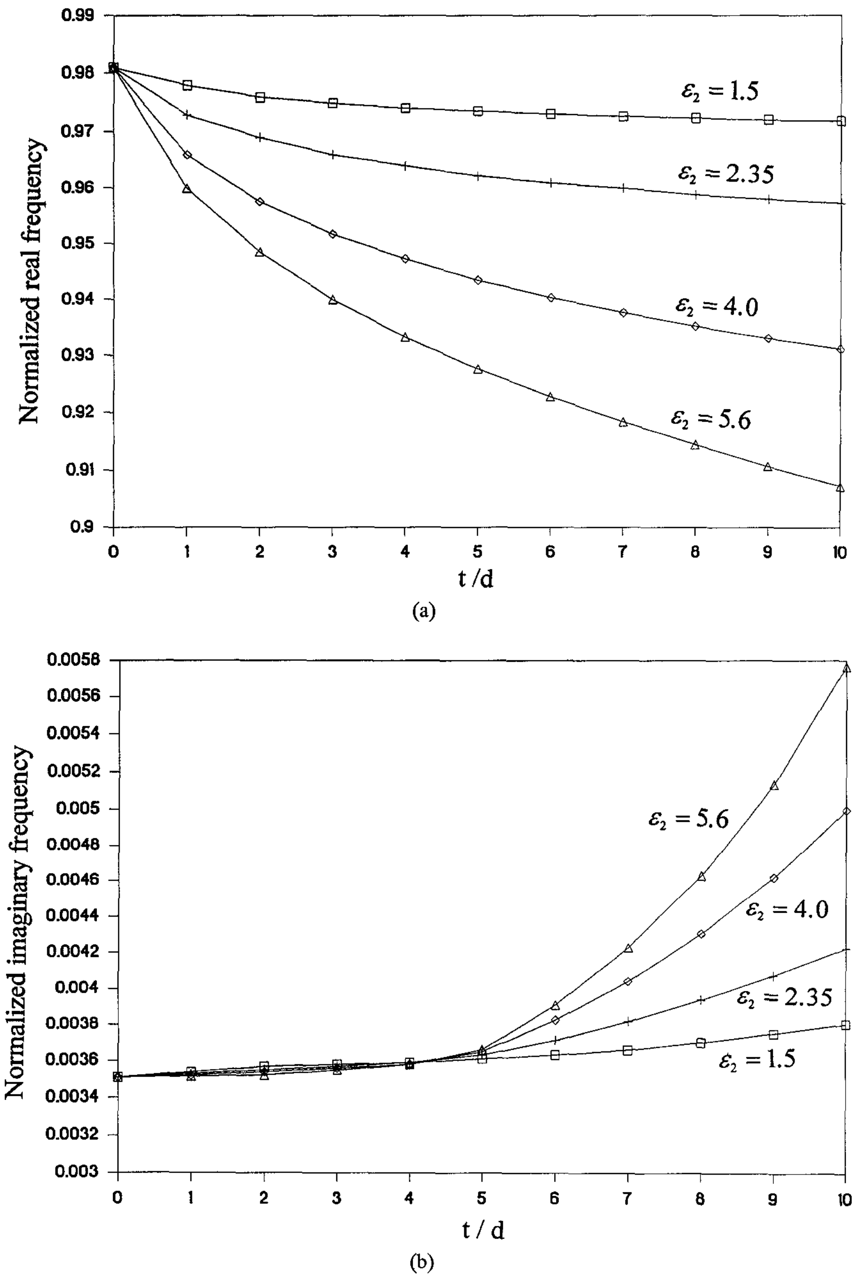

Fig. 6. Normalized complex resonant frequency of a superstrate-loaded rectangular patch versus the superstrate thickness; $\varepsilon_1 = 2.35$, $\varepsilon_2 = 1.5$, 2.35, 4, and 5.6; $a = 6$ cm, $b = 5$ cm, $d = 0.1$ cm. (a) Real part of resonant frequency. (b) Imaginary part of resonant frequency.

that of the substrate. The TM_{01} mode for the superstrate-loaded rectangular microstrip structure is shown to be an efficiently radiating mode.

REFERENCES

[1] W. C. Chew and Q. Liu, "Resonance frequency of a rectangular microstrip patch," *IEEE Trans. Antennas Propagat.*, vol. AP-36, pp. 1045–1056, 1988.

[2] A. Bhattacharyya and T. Tralman, "Effects of dielectric superstrate on patch antennas," *Electron. Lett.*, vol. 24, pp. 356–358, 1988.

[3] K. M. Luk, W. Y. Tam, and C. L. Yip, "Analysis of circular microstrip antennas with superstrate," *IEE Proc.*, vol. 136, pt. H, pp. 261–262, 1989.

[4] K. L. Wong, W. S. Chen, and W. L. Huang, "The absorption and coupling of an electromagnetic wave incident on a microstrip circuit with superstrate," *IEEE Trans. Electromagn. Compat.*, vol. EMC-34, pp. 17–22, 1992.

[5] R. F. Harrington, *Field Computation by Moments Methods.* New York: Macmillan, 1968.

[6] E. H. Newman and D. Forrai, "Scattering from a microstrip patch," *IEEE Trans. Antennas Propagat.*, vol. AP-35, pp. 245–251, 1987.

[7] P. B. Katehi and N. G. Alexopoulos, "On the effect of substrate thickness and permittivity on printed circuit dipole properties," *IEEE Trans. Antennas Propagat.*, vol. AP-31, pp. 34–39, 1983.

[8] N. G. Alexopoulos, P. B. Katehi, and D. B. Rutledge, "Substrate optimization for integrated circuit antennas," *IEEE Trans. Microwave Theory Tech.,* vol. MTT-31, pp. 550–557, 1983.

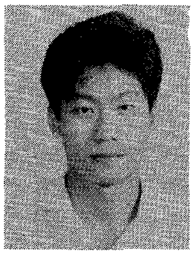

Jeen-Sheen Row was born in Miaoli, Taiwan, Republic of China, in 1967. He received the B.S. degree in electrical engineering from Tamkang University, Taipei, Taiwan, in 1989.

Since 1990 he has been working toward the Ph.D. degree in the Department of Electrical Engineering at the National Sun Yat-Sen University, Kaohsiung. His current research interests are in antenna theory and design, and EM wave propagation.

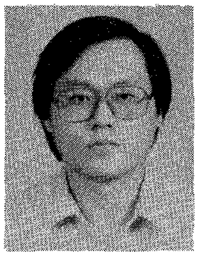

Kin-Lu Wong (M'91) was born in Tainan, Taiwan, in 1959. He received the B.S. degree in electrical engineering from National Taiwan University, Taipei, Taiwan, in 1981, and the M.S. and Ph.D. degrees in electrical engineering from Texas Tech University, Lubbock, in 1984, and 1986, respectively.

From 1986 to 1987 he was a Visiting Scientist with Max-Planck-Institut fuer Plasmaphysik in Munich, Germany. In 1987 he was with the Department of Electrical Engineering at National Sun Yat-Sen University, Kaohsiung, Taiwan, where he became a Professor in 1991. His research interests include electromagnetic theory, antenna design, and plasma science.